Three Different Ways of White Residual Generation To Detect Faults in Precise Real-Time DGPS/DGNSS

Ju-Young Shim*, Hyung Keun Lee*, Heung Kyu Lee**, Binghao Li***, Ben K. H. Soon***

School of Avionics and Telecommunication., Korea Aerospace University, Korea

Department of Civil Engineering, Changwon National University, Korea

School of Surveying and Spatial Information Systems, UNSW, Australia

School of Aerospace, Mechanical and Mechatronic Engineering, University of Sydney, Australia

Abstract

Fault detection and isolation is one of the most important issues in implementing GPS/GNSS technology. To categorize for modeling and analysis, there are largely two types of faults: hard faults and soft faults. Hard faults correspond to abrupt changes and soft faults correspond to slow changes in measurement residuals. Since a soft fault can hide behind the filter′s state estimate that slowly diverges, it is not an easy task to detect a soft fault even for a static receiver.

As evidenced by the previous research works on non-snapshot methods, a good fault detector need to generate measurement residual sequences internally. The measurement residual sequences need to be white if no fault exists and non-white if a fault exists. If the detector satisfied this condition, the well-known chi-square statistics can be conveniently utilized with various decision statistics in a standardized way.

Since most GPS/GNSS applications are involved with moving receivers, it is desirable to design a method to detect soft faults in real-time kinematic conditions. In this paper, three different methods to generate the channelwise white residual sequences in real-time kinematic conditions are introduced and their characteristics are evaluated by experiment data. The effectiveness of the three channelwise white residual sequence generation schemes under multiple synchronous faults and soft faults is demonstrated by utilizing real measurements in the simulated real-time mode.

I. INTRODUCTION

As widely known, the focus of research activities on GNSS is moving from accuracy to reliability. To improve reliability, various research works has been performed on the fault detection and isolation (FDI) methodology. The FDI capability is very important especially when the receivers are moving since undetected faults may lead to hazardous accidents.

The FDI method in GNSS can be largely categorized into the snapshot method and the sequential method [1-5]. The snapshot method utilizes the measurements of the same time instant but with respect to different satellites. The sequential method utilizes the time-sequences of measurements where each time-sequence corresponds to each visible satellite. To process the measurement sequence, the sequential methods utilize various variations of estimators or filters to generate the measurement residual sequences. The measurement residual is the difference between the raw measurement and the filter's estimate of the equivalence to the raw measurement based on the system model and the *a priori* state estimate. The measurement residual is also called as the indirect measurement as compared with the direct measurement which is the unmodified raw measurement.

Though computationally simple to implement, the snapshot method cannot overcome the shortcomings of channel redundancy and the difficulty of indentifying synchronous multiple faults. Thus, in spite of the computational burden, the sequential method is more recommended to the safety critical applications.

For the effectiveness of the FDI, the correct decision whether there is no fault or there are faults plays a crucial role. Furthermore, the fault decision needs to be simple to implement and easily related to many meaningful statistics. If a test statistic satisfies the zero-mean white Gaussian distribution in normal condition and shifted Gaussian distribution in abnormal condition, its square corresponds to the centralized chi-square distribution and the non-centralized chi-square distribution, respectively. Since the statistical tables for the Gaussian and chi-square distributions are well known and they are connected to many existing analysis results on the FDI, a test statistic is usually desired to satisfy a white Gaussian distribution or a chi-squared distribution by simple computation.

By the rationale, the FDI problem can be partially reduced to the topic on how efficiently a statistical sequence can be generated that is white Gaussian in normal conditions and shifted and distorted Gaussian in fault conditions. The most well known method to generate white residual sequence is the implement the Kalman filter [6,7]. Then, a white Gaussian sequence can be generated by the indirect measurements of the Kalman filter as the differences between the actual measurement and the estimated measurements by the filter's *a priori* state estimate at every instants.

As reported in [8], the GPS Kalman filter that utilizes the conventional Kalman filter algorithm based on a specific dynamic model cannot provide accurate position estimates when the receiver experiences a violation of the specific dynamic model. To overcome this problem, multiple model filters [9,10] may be utilized. But it will lead to computationally burdensome algorithm. As widely known, to achieve the maximum allowable accuracy in real-time kinematic GPS/GNSS, the carrier-smoothed-code filter is the most recommended method.

As recently reported [11, 12], it is not the Kalman gain but the Hatch gain that generates a white residual sequence in range-domain (RD) carrier-smoothed-code filtering. Extending the range-domain result, the position-domain (PD) Hatch filter was also proposed to prevent the information loss in frequent changes of visible satellites. It was shown that the position-domain Hatch filter also generates a white residual sequence. In addition to the RD and PD Hatch filters, a different method to generate a white residual sequence is reported in [13, 14] where the test statistics are especially useful detecting multipath-affected channels in real-time kinematic positioning.

In this paper, the three different methods to generate the channelwise white residual sequences are summarized and compared by a set of experiment data. The effectiveness of the channelwise white residual sequence generation schemes in FDI under multiple synchronous faults and soft faults is demonstrated.

II. Channelwise White Gaussian Residual Sequence Generation

If a user's receiver and a reference receiver are located close by or dual-frequency receivers are used, the common error sources such as the satellite-oriented error, ionospheric delay, and tropospheric delay can be effectively eliminated. The corrected pseudorange $\tilde{\rho}_{j,k}$ and carrier phase $\tilde{\phi}_{j,k}$ with respect to the j-th satellite at the k-th epoch can be modeled as:

$$\tilde{\rho}_{j,k} = e_{j,k}^T(x_{j,k} - x_{u,k}) + b_{u,k} + v_{j,k}$$

$$\tilde{\phi}_{j,k} = e_{j,k}^T(x_{j,k} - x_{u,k}) + b_{u,k} + n_{j,k} + \lambda N_j$$

$$\begin{bmatrix} v_{j,k} \\ v_{j,k+1} \\ v_{j+1,k} \\ n_{j,k} \\ n_{j,k+1} \\ n_{j+1,k} \end{bmatrix} \sim \left(\begin{bmatrix} 0 \\ 0 \\ 0 \\ 0 \\ 0 \\ 0 \end{bmatrix}, \begin{bmatrix} r_\rho & 0 & 0 & 0 & 0 & 0 \\ 0 & r_\rho & 0 & 0 & 0 & 0 \\ 0 & 0 & r_\rho & 0 & 0 & 0 \\ 0 & 0 & 0 & r_\phi & 0 & 0 \\ 0 & 0 & 0 & 0 & r_\phi & 0 \\ 0 & 0 & 0 & 0 & 0 & r_\phi \end{bmatrix} \right) \quad (1)$$

where

$e_{j,k}$: Line of Sight (LOS) vector from the receiver to the j-th satellite at the k-th epoch

$x_{j,k}$: Earth-Centered Earth-Fixed (ECEF) position of the j-th satellite at the k-th epoch

$x_{u,k}$: ECEF receiver position at the k-th epoch $b_{u,k}$: receiver clock bias at the k-th epoch

N_j: unresolved integer ambiguity

$v_{j,k}$, $n_{j,k}$: noise terms in the code and carrier measurements

r_ρ, r_ϕ: uniform noise strength values of code and carrier measurements

$\sim (m, P)$: Gaussian distribution with the mean m and the covariance P

From now on, for notational convenience, the symbol X_k will be used to denote the true state vector, that is composed of the three-dimensional position sub-vector $x_{u,k}$ and the receiver clock bias $b_{u,k}$:

$$X_k := \begin{bmatrix} x_{u,k} \\ \cdots \\ b_{u,k} \end{bmatrix} \tag{2}$$

Related to the true state vector X_k, the symbols $\bar{X}_k$, $\delta\bar{X}_k$, $\bar{P}_k$, $\hat{X}_k$, $\delta\hat{X}_k$, and $\hat{P}_k$ are used to represent the *a priori* state estimate, *a priori* estimation error, *a priori* error covariance matrix, *a posteriori* state estimate, *a posteriori* estimation error, and *a posteriori* error covariance matrix at the k-th step for all the filters considered, respectively:

$$\bar{X}_k = \begin{bmatrix} \bar{x}_{u,k} \\ \cdots \\ \bar{b}_{u,k} \end{bmatrix}, \quad \delta\bar{X}_k := \bar{X}_k - X_k = \begin{bmatrix} \delta\bar{x}_{u,k} \\ \cdots \\ \delta\bar{b}_{u,k} \end{bmatrix}, \quad \delta\bar{X}_k \sim (O, \bar{P}_k),$$

$$\hat{X}_k = \begin{bmatrix} \hat{x}_{u,k} \\ \cdots \\ \hat{b}_{u,k} \end{bmatrix}, \quad \delta\hat{X}_k := \hat{X}_k - X_k = \begin{bmatrix} \delta\hat{x}_{u,k} \\ \cdots \\ \delta\hat{b}_{u,k} \end{bmatrix}, \quad \delta\hat{X}_k \sim (O, \hat{P}_k). \tag{3}$$

To denote the true displacement information, the symbol ΔX_k will be used:

$$\Delta X_k := X_{k+1} - X_k = [(\Delta x_{u,k})^T \vdots \Delta b_{u,k}]^T \tag{4}$$

The symbols I and O will be used to notate identity and zero matrices of appropriate dimension. If necessary, their dimensions are explicitly given using subscripts.

A. *Range-Domain Hatch Filter*

The first method to generate a channelwise white Gaussian residual sequence is to use the well-known RD Hatch filter summarized as follows.

Initialization:

$\alpha_{j,k0} = 0$, $\beta_{j,k0} = 1$, $\hat{\rho}_{j,k0} = \tilde{\rho}_{j,k0}$, $\hat{R}_{j,k0} = r_{\rho}$

k_0: filter initialization time index $(k > k_0)$ (5)

Time-Propagation:

$$\bar{\rho}_{j,k+1} := \hat{\rho}_{j,k} + (\tilde{\phi}_{j,k+1} - \tilde{\phi}_{j,k})$$

$$\bar{v}_{j,k+1} := \hat{v}_{j,k} + (\tilde{\phi}_{j,k+1} - \tilde{\phi}_{j,k})$$

$$\bar{R}_{j,k+1} = \hat{R}_{j,k} + 2\beta_{j,k} r_{\Phi} \tag{6}$$

Measurement Update:

$$\beta_{j,k} = 1/k$$

$$\hat{v}_{j,k} = (1-\beta_{j,k})\bar{v}_{j,k} + \beta_{j,k} v_{j,k} = \bar{v}_{j,k} - \beta_{j,k}(\bar{v}_{j,k} - v_{j,k})$$

$$\hat{R}_{j,k} = (1-\beta_{j,k})^2 \bar{R}_{j,k} + (\beta_{j,k})^2 r_{\rho} \tag{7}$$

It is analytically shown in [12] that the sequence of the measurement residual $\{\vartheta_{j,k}\}_{k=1,2,3,\cdots}$ with respect to the j-th satellite is white.

$$\vartheta_{j,k} = \tilde{\rho}_{j,k} - \bar{\rho}_{j,k} \tag{8}$$

B. *Position-Domain Hatch Filter*

The indirect measurement $z_{j,k}$ with respect to $\delta\bar{X}_k$ for measurement update for PD filtering is formed by the following equation:

$$z_{j,k} = \tilde{\rho}_{j,k} - e_{j,k}^T (x_{j,k} - \bar{x}_{u,k}) - \bar{b}_{u,k} \tag{9}$$

Then, the indirect measurement z_k^j satisfies the condition:

$$z_{j,k} = h_{j,k}\delta\bar{X}_k + v_{k,j}$$

$$h_{j,k} := [e_{j,k}^T \;\vdots\; -1] \tag{10}$$

In PD filters, all the channelwise scalar measurements participate in position estimation concurrently, as they are acquired. Thus, vector notation is more convenient in describing PD filters. The indirect measurement vector Z_k to update the position estimate $\bar{X}_k$ from to $\hat{X}_k$ is written as follows:

$$Z_k = H_k \delta\overline{X}_k + v_k, \ \ v_k \sim (O_{J\times 1}, r_\rho I_{J\times J}) \tag{11}$$

where

$$Z_k := \begin{bmatrix} z_{1,k} \\ z_{2,k} \\ \vdots \\ z_{J,k} \end{bmatrix}, \quad H_k := \begin{bmatrix} h_{1,k} \\ h_{2,k} \\ \vdots \\ h_{J,k} \end{bmatrix}, \quad v_k := \begin{bmatrix} v_{1,k} \\ v_{2,k} \\ \vdots \\ v_{J,k} \end{bmatrix}$$

$$z_{j,k} := \tilde{\rho}_{j,k} - e_{j,k}^T (x_{j,k} - \overline{x}_{u,k}) - \overline{b}_{u,k} = h_{j,k} \delta\overline{X}_k + v_{j,k}$$

$$h_{j,k} := [e_{j,k}^T \ \vdots \ -1]$$

J : number of visible satellites (12)

Similarly, the indirect measurement vector Ω_{k+1} to propagate $\hat{X}_k$ in time toward $\overline{X}_{k+1}$ is written as:

$$\Omega_{k+1} = H_{k+1} \Delta X_k + W_{k+1}$$

$$W_{k+1} = -\Delta H_k \delta\hat{X}_k - n_{k+1} + n_k, \quad n_k \sim (O_{J\times 1}, r_\Phi I_{J\times J}) \tag{13}$$

where

$$\Omega_{k+1} := \begin{bmatrix} \omega_{1,k+1} \\ \omega_{2,k+1} \\ \vdots \\ \omega_{J,k+1} \end{bmatrix}, \ W_{k+1} := \begin{bmatrix} w_{1,k+1} \\ w_{2,k+1} \\ \vdots \\ w_{J,k+1} \end{bmatrix}, \ n_k := \begin{bmatrix} n_{1,k} \\ n_{2,k} \\ \vdots \\ n_{J,k} \end{bmatrix}$$

$$\Delta H_k := H_{k+1} - H_k$$

$$\begin{aligned} \omega_{j,k+1} &:= e_{j,k}^T \Delta x_{j,k} + \Delta e_{j,k}^T (x_{j,k+1} - \hat{x}_{u,k}) - (\tilde{\phi}_{j,k+1} - \tilde{\phi}_{j,k}) \\ &= h_{j,k+1} \Delta X_k + w_{j,k+1} \end{aligned}$$

$$w_{j,k+1} := -\Delta e_{j,k}^T \delta\hat{x}_{u,k} - n_{j,k+1} + n_{j,k} \tag{14}$$

Based on Z_k and Ω_{k+1} in Eqs. (11) and (13), the second method to generate a channelwise white Gaussian residual sequence can be summarized as shown in Table 1 that corresponds to the PD Hatch filter.

In Table 1, the channel selection matrix Γ_k is used to consider abrupt satellite inclusions and outages. The selection matrix Γ_k consists of 0’s and 1’s where 1 denotes the measurement that is valid at both the k and $(k-1)$-th step, simultaneously. Thus, the selection matrix Γ_k maps from the full- dimensional measurement vector Ω_k and Z_k that considers all the channels to the reduced measurement vector Y_k^*.

TABLE 1 POSITION-DOMAIN HATCH FILTER

Initialization:
$H_{k0}^* = \Gamma_{k0} H_{k0}$
$\hat{X}_{k0} = E[X_{k0} \mid \Gamma_{k0} \tilde{\rho}_{k0}]$, $\quad \hat{P}_{k0} = r_\rho [(H_{k0}^*)^T H_{k0}^*]^{-1}$
Time-Propagation:
$H_{k+1}^* = \Gamma_{k+1} H_{k+1}$, $\quad H_k^p = \Gamma_{k+1} H_k$, $\quad \Omega_{k+1}^* = \Gamma_{k+1} \Omega_{k+1}$
$U_{k+1}^* = [(H_{k+1}^*)^T H_{k+1}^*]^{-1} (H_{k+1}^*)^T$
$\overline{X}_{k+1} = \hat{X}_k + U_{k+1}^* \Omega_{k+1}^*$
$\overline{P}_{k+1} = U_{k+1}^* \left\{ H_k^p \hat{P}_k (H_k^p)^T + r_\phi \begin{bmatrix} 2I - H_k^p \left(I - K_k^* H_k^*\right) U_k^* \Gamma_k \Gamma_{k+1}^T \\ - \Gamma_{k+1} \Gamma_k^T (U_k^*)^T \left(I - K_k^* H_k^*\right)^T (H_k^p)^T \end{bmatrix} \right\} (U_{k+1}^*)^T$
Measurement Update:
$K_k^* = \left\{ \overline{P}_k - r_\phi \left[(H_k^*)^T H_k^* \right]^{-1} \right\} (H_k^*)^T \left[H_k^* \overline{P}_k (H_k^*)^T + r_\rho I \right]^{-1}$
$Z_k^* = \Gamma_k Z_k$
$\hat{X}_k^* = \overline{X}_k^* - K_k^* Z_k^*$,
$\hat{P}_k^* = \left(I - K_k^* H_k^*\right) \overline{P}_k^s \left(I - K_k^* H_k^*\right)^T + r_\rho K_k^* (K_k^*)^T$

It is analytically shown in [12] that the sequence of the measurement residual $\{z_{j,k}\}_{k=1,2,3,\cdots}$ with respect to the j-th satellite as shown in Eq. (12) is also a white Gaussian sequence.

C. Orthogonalized Successive-Time Double-Differences

The last method to obtain a white Gaussian residual sequence starts by forming a successive-time double-difference (STDD) that is the difference between the incremental carrier-phase and pseudorange measurements.

$$d_i^j = (\tilde{\rho}_i^j - \tilde{\rho}_{i-1}^j) - (\tilde{\Phi}_i^j - \tilde{\Phi}_{i-1}^j) \qquad (15)$$

where

$$\begin{bmatrix} v_i^j \\ v_l^j \end{bmatrix} \sim \left(O, \begin{bmatrix} \Lambda_\rho & -\frac{1}{2}\Lambda_\rho \\ -\frac{1}{2}\Lambda_\rho & \Lambda_\rho \end{bmatrix} \right) \quad \text{if } \ l = i \pm 1$$

$$\sim \left(O, \begin{bmatrix} \Lambda_\rho & 0 \\ 0 & \Lambda_\rho \end{bmatrix} \right) \qquad \text{if } \ l \neq i \pm 1$$

$$\Lambda_\rho := 2(r_\rho + r_\Phi)\,. \tag{16}$$

Due to the correlation between noise terms in successive epochs, as shown in Eq. (1), the subsequent STDDs d_i^j and d_{i+1}^j are correlated, as shown in Eq. (16). To eliminate the correlation, a stochastic orthogonalization is applied to the STDD sequence to generate the following orthogonalzed STDD (OSTDD) sequence [14]:

$$\bar{d}_{k-B+1}^{\,j} = d_{k-B+1}^{\,j}$$

$$\bar{d}_i^{\,j} = d_i^{\,j} + \frac{1}{2}\frac{\Lambda_\rho}{\bar{\Lambda}_{i-1}^j}\bar{d}_{i-1}^{\,j}\,, \ \ i = k-B+2,\, k-B+3,\, \cdots,\, k \tag{17}$$

As a result of the stochastic orthogonalization, the OSTDD sequence $\left\{\bar{d}_i^{\,j}\right\}_{i=k-B+1,\, k-B+2,\, ...,\, k}$ becomes white Gaussian.

$$\begin{bmatrix} \bar{d}_k^{\,j} \\ \bar{d}_{k-1}^{\,j} \\ \bar{d}_{k-2}^{\,j} \\ \vdots \\ \bar{d}_{k-B+1}^{\,j} \end{bmatrix} \sim \left(O, \begin{bmatrix} \bar{\Lambda}_k^j & & & & O \\ & \bar{\Lambda}_{k-1}^j & & & \\ & & \bar{\Lambda}_{k-2}^j & & \\ & & & \ddots & \\ O & & & & \bar{\Lambda}_{k-B+1}^j \end{bmatrix} \right) \tag{18}$$

where

$$\bar{\Lambda}_{k-B+1}^j = \Lambda_\rho$$

$$\bar{\Lambda}_i^j = \Lambda_\rho - \frac{1}{4}\frac{\Lambda_\rho{}^2}{\bar{\Lambda}_{i-1}^j}\,, \ \ i = k-B+2,\, k-B+3,\, \cdots,\, k\,. \tag{19}$$

III. EXPERIMENT

To compare the three white residual generation methods, a set of experiment data was gathered. For the experiment, a vehicle was run around a semi-urban area. During the run, all the raw measurements of the reference and rover were logged. The logged measurements in the Receiver Independent Exchange (RINEX) format was applied to the GAFAS software package with wide-lane combinations in the simulated real-time mode. GAFAS is abbreviation of the GNSS algorithm for accuracy and safety. It consists of approximately 200 software modules whose functionalities are grouped as shown in Fig. 1. To extract the reference trajectory, a commercial software package for Carrier-phase Differential GPS (CDGPS) was utilized. Since the reference trajectory is based on the resolved integer ambiguity in the differenced carrier phase measurements, its typical accuracy is in the order of cm.

The experiment lasted 2000 seconds during which the vehicle repeated following a rectangular path. As can be seen later, large multipath errors seem to occur near 200, 400, 1600, and 1800 seconds, respectively. In addition to the multipath errors, intentional jump- and ramp-type faults are injected as shown in Table 2 and Fig. 2. As shown, multiple faults are injected at to the different channels at the same instants to simulate the multiple synchronous faults.

Fig. 3 shows the residual sequences in time-domain and its auto-correlation profiles when there is no fault. In both the left and right sides of Fig. 3, the upper plots correspond to the RD Hatch filter, the middle plots correspond to the PD Hatch filter, and the lower plots correspond to the OSTDD. As shown in the figure, the three different methods generate very similar residual sequences. It is also shown that the maximum auto-correlation value is shown like a jump as in the case of the ideal auto-correlation function. Also, it can be seen that the auto-correlation profile is not exactly flat due to uneliminated atmospheric errors and weak multipath errors.

Fig. 4 shows the residual sequences in time-domain and Fig. 5 shows the auto-correlation profiles when there are faults. In Fig. 4 and Fig. 5, left plots correspond to the case where jump-type hard faults are injected and the right plots correspond to the case where a ramp-type soft fault is injected. It can be seen that the injected faults are clearly seen in the generated residual sequences. As shown in Fig. 5, the hard faults generate many intermittent small peaks and the soft fault makes the maximum value not as a jump but as a peak of a delta shape .

Since the fault occurrence can be clearly detected by any of the three residual generation methods as shown in Figs. 3, 4, and 5, the fault-affected measurements can be effectively eliminated or de-weighted to minimize the position estimation error. If the channelwise fault detection and isolation structure like that of the GAFAS, the estimation error can be largely reduced from that shown in Fig. 6 to that shown in Fig. 7. The large error distance values observed at 200, 1600, and 1800 seconds are not due to the estimation error but due to the reference information error as magnified in Fig. 8. By comparing Fig. 6 and Fig. 7, the accuracy and reliability improvement is more apparent when there are soft faults that are more difficult to detect than hard faults.

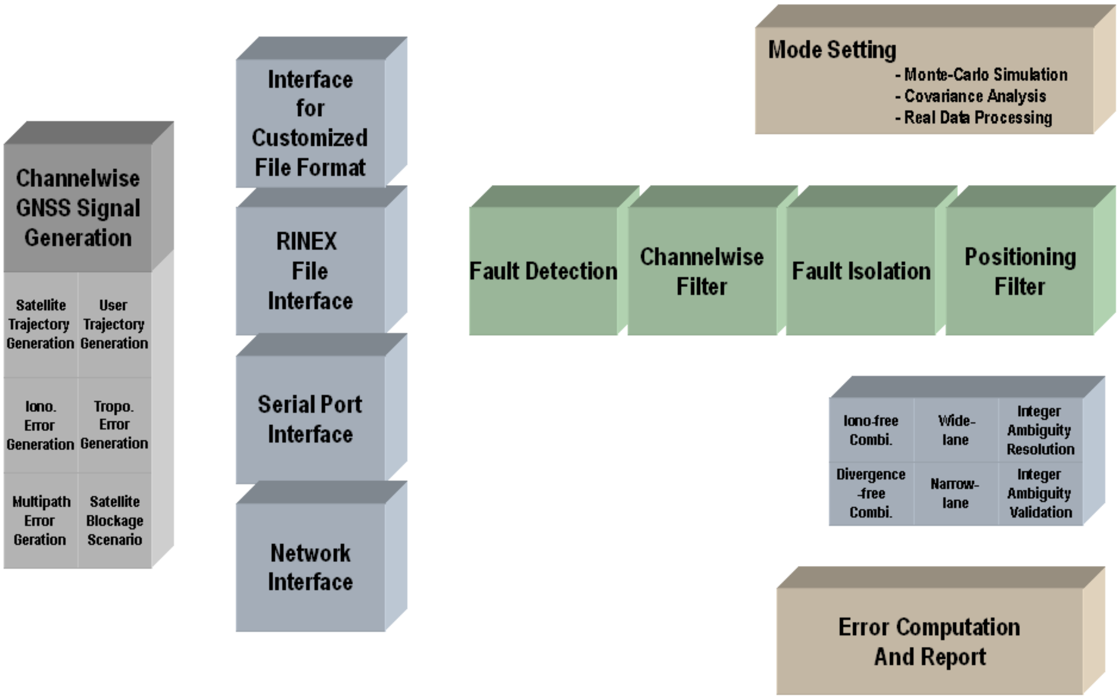

Fig. 1 Functionalities of the GAFAS software package used in the experiment

TABLE 2 SUMMARY OF INJECTED FAULTS

time (sec)	50	70	90	200	300	400	500	1200	1300	1850
affected SV channel ID	3	11 15	3 19	8 11	15 16 19	3 19	8 11	15 16 19	3 19	8 11
duration (sec)	10	10	10	10	10	10	10	10	10	150
fault type (Jump/Ramp)	J	J	J	J	J	J	J	J	J	R
magnitude(m) / slope(m/sec)	2	2	2	2	2	2	2	2	2	0.1

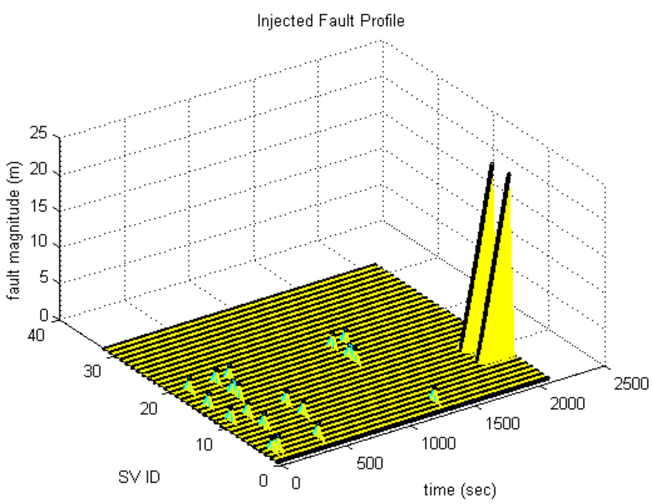

Fig. 2 Injected fault profile

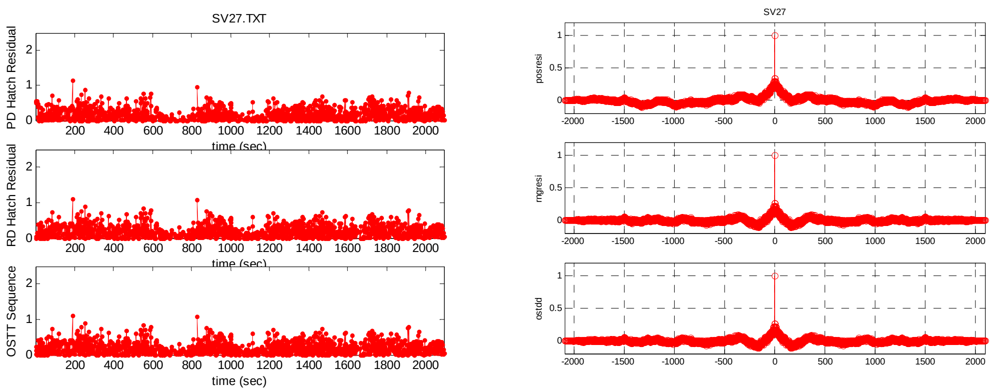

Fig. 3 Residual sequences (left) and their auto-correlation profiles (right) without fault

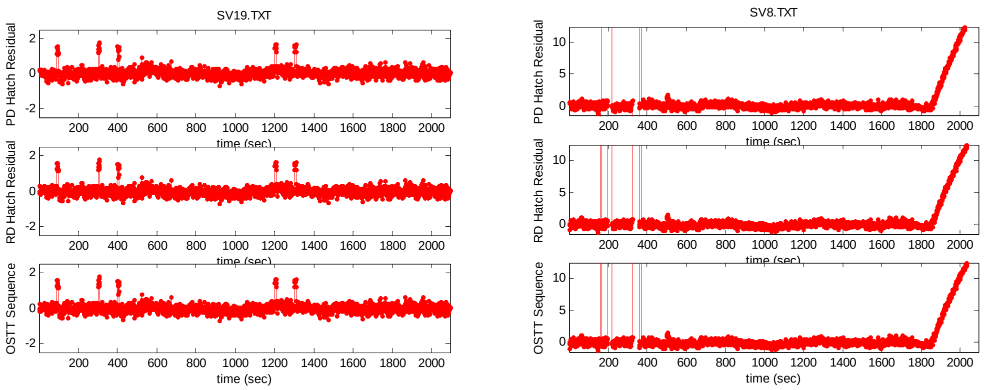

Fig. 4 Residual sequences affected by intermittent hard faults (left) and soft fault (right)

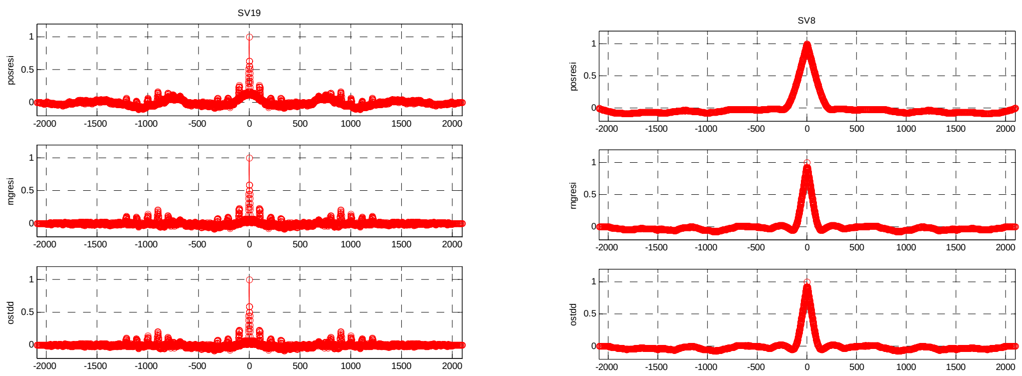

Fig. 5 Auto-correlation profiles affected by intermittent hard faults (left) and soft fault (right)

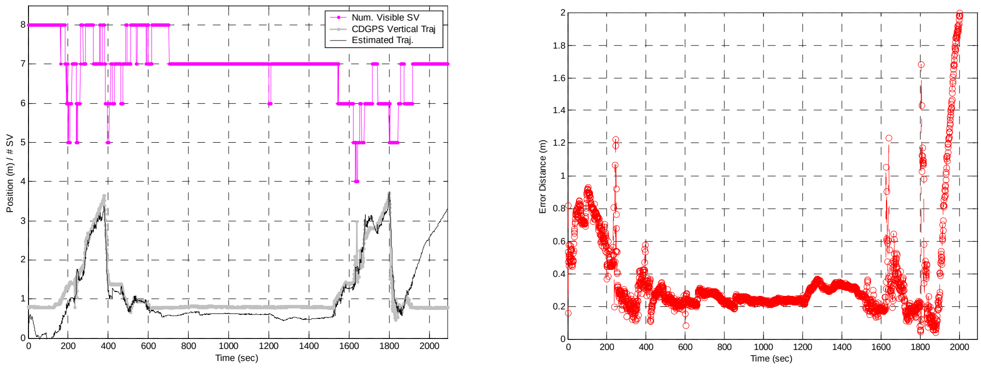

Fig. 6 Number of valid satellites, the reference and estimated height values (left), and the error distance between the reference and estimated trajectories (right) when there is no fault detection and isolation scheme

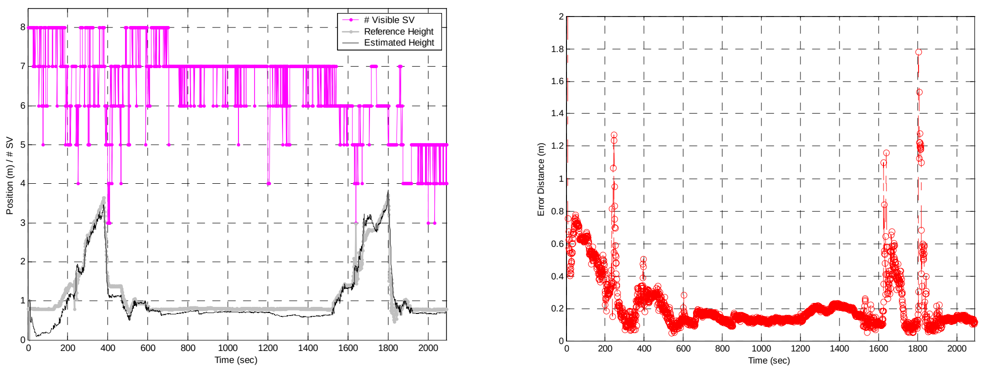

Fig. 7 Number of valid satellites, the reference and estimated height values (left), and the error distance between the reference and estimated trajectories (right) when the residual sequence of the position-domain Hatch filter is utilized for fault detection and isolation scheme

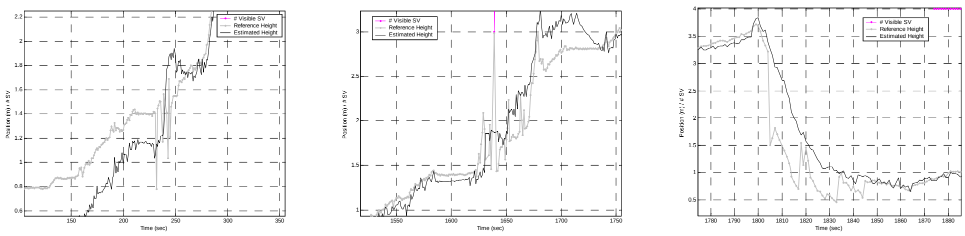

Fig. 8 Magnified plots near 200, 1600, and 1800 seconds where large error distance values between the reference and estimated trajectories appear.

IV. CONCLUSION

To detect and isolate synchronous soft and hard faults in real-time kinematic applications, three different methods to generate the channelwise white residual sequences are introduced and their characteristics are evaluated by the time-domain profile and the auto-correlation function of each residual. The effectiveness of the three channelwise white residual sequence generation schemes is demonstrated by utilizing real measurements in the simulated real-time mode.

References

[1] M. A. Sturza and A. K. Brown, “Comparison of fixed and variable threshold RAIM algorithms,” *Proceeding of Third International Technical Meeting of ION*, pp. 439-443, 1990.

[2] R. G. Brown and G. Y. Chin, “GPS RAIM: Calculation of threshhold and protection radius using chi-square methods - a geometric approach,” *Global Positioning System*, Vol. V, The Institute of Navigation, pp. 155-179, 1997.

[3] Y. C. Lee, “Analysis of range and position comparison methods as a means to provide GPS integrity in the user receiver,” *Proceedings of ION Annual Meeting*, Seattle, WA, pp. 1-4, June, 1986.

[4] E. Page, “Continuous inspection schemes,” *Biometrika*, 41, pp. 100-115, 1954

[5] C. Ogaja, “On-line GPS integrity monitoring and deformation analysis for structural monitoring applications,” *14th Int. Tech. Meeting of ION*, Salt Lake City, Utah, 11-14 September, 989-999, 2001

[6] N. A. Carlson, "Federated square root filter for decentralized parallel processes," *IEEE Transactions on Aerospace and Electronic Systems*, vol. 26, no. 3, pp. 517-525, 1990

[7] T. Kailath, A. H. Sayed, and B. Hassibi, Linear Estimation, Prentice Hall, 2000

[8] H. K. Lee, C. Rizos, and G. I. Jee, "Design of kinematic DGPS filters with consistent error covariance information", *IEE Proceedings - Radar, Sonar and Navigation*, Vol. 151, No. 6, pp.382-388, 2004

[9] H.A.P Blom and Y. Bar-Shalom, “The interacting multiple model algorithm for systems with markovian switching coefficients,’’ *IEEE Trans. Automatic Control*, vol. 33 , no. 8, pp. 780-783, Aug. 1988.

[10] Johnston, L.A.; Krishnamurthy, V. “An improvement to the interacting multiple model (IMM) algorithm,”*IEEE Tr. Signal Processing*, Vol. 49, No. 12, pp. 2909 – 2923, 2001

[11] H. K. Lee and C. Rizos, "A New Recursive Carrier-Smoothed-Code Filter for differential Global Navigation Satellite Sytems," *Proceedings of 11th IAIN World Congress: Smart Navigation - Systems and Services* -, Berlin, Oct. 2003

[12] H. K. Lee and C. Rizos, "Position-Domain Hatch Filter for Kinematic Differential GPS/GNSS", *IEEE Transactions on Aerospace and Electronic Systems*, Accepted for publication, 2007

[13] H. K. Lee, J. G. Lee, and G. I. Jee, “An Efficient GPS Receiver Algorithm for Channelwise Multipath Detection and Real-Time Positioning”, *Proceedings of Institute of Navigation 2002 National Technical Meeting*, San Diego, CA, January 28-30, 2002

[14] H. K. Lee, J. G. Lee, and G. I. Jee, “GPS Multipath Detection Based on Successive-Time Double-Differences”, *IEEE Signal Processing Letters*, Vol. 11, No. 3, pp. 316-319, 2004